Astro2020 APC White Paper:
The Advanced Particle-astrophysics Telescope (APT)

Consideration areas: Small and Medium Space-based Project

Authors: J.H. Buckley[1], L. Bergström[2], W.R. Binns[1], J. Buhler[1], Wenlei Chen[3], M. Cherry[4], S. Funk[5], D. Hooper[6], J. Mitchell[7], G. De Nolfo[7], S. Al Nussirat[4], S. Profumo[8], B. Rauch[1], D. Stern[9], G. Varner[10], S. Wakely[11], A. Zink[5]

Contact: James Buckley, Washington University, St. Louis, MO 63130
(e-mail: buckley@wustl.edu)

Abstract

We propose a mission concept for a space-based gamma-ray and cosmic-ray explorer known as the Advanced Particle-astrophysics Telescope (APT). We consider two realizations of the instrument; a 3m×3m detector that would fall just under the $500M threshold for a small instrument, and a larger 3m×6m instrument that would be a candidate for a probe-class mission. The instrument design was driven by two scientific objectives: (1) to confirm or rule out the thermal WIMP dark matter paradigm and (2) to promptly localize the electromagnetic counterparts of gravity-wave/neutron-star mergers. These goals motivate a gamma-ray instrument with ten times the sensitivity of Fermi at GeV energies, simultaneously providing sub-degree MeV transient localization over the largest possible field of view. A Sun–Earth Lagrange orbit for the instrument would remove Earth obscuration, allowing a view of the entire sky. The very large area needed to achieve this sensitivity coupled with a high-Earth orbit dictate the use of an electromagnetic calorimeter with limited depth (<6 radiation lengths) to reduce mass. Such an instrument would also be a powerful cosmic-ray detector capable of measuring the elemental abundances of very rare, ultra-heavy r-process cosmic-ray nuclei for material originating outside our solar system, connecting to the n-star merger science. With the addition of foam radiators, the CsI detectors could detect the transition radiation X-rays from very-high-energy light cosmic rays, specifically Boron and Carbon, needed to differentiate models of cosmic ray propagation of importance to indirect dark matter detection. The APT detector design would incorporate 20 layers of 5mm thick CsI:Na with crossed wavelength shifting fiber (WLS fiber) readout, interspersed with 20 $x - y$ scintillating optical fiber tracker (SOFT) layers using interleaved 1.5mm round scintillating fibers. The 3m×3m×2.5m detector volume consisting of passive plastic scintillating fibers and CsI crystals would be read out on the sides with SiPM photodetectors and analog-pipeline waveform digitizers. Detailed simulations and laboratory measurements show that the APT instrument could achieve ~10 times the sensitivity of the *Fermi* LAT for pair-events from 60 MeV–TeV gamma-rays and provide more than an order of magnitude improvement in sensitivity over any other proposed gamma-ray experiment in the MeV energy range with prompt GRB source localization to better than 1° uncertainty. Likewise, the cosmic-ray detector would improve statistics on rare heavy elements and rare very-high-energy lighter nuclei by orders of magnitude compared to any extant experiment.

[1]Washington University (WU), [2]Stockholm U., [3]U. Minnesota, [4]Louisianna State University, [5]Erlangen Center for Astroparticle Physics, [6]Fermi National Accelerator Laboratory,[7]Goddard Space Flight Center, [8]University of California, Santa Cruz, [9]Jet Propulsion Laboratory, [10]U. Hawaii, [11]U. Chicago

1 Introduction

We propose a small (<$500M) to midsize ($\sim$ 1G$) mission aimed at two key scientific objectives: (1) detecting or ruling out thermal WIMP dark matter (DM) over the entire natural parameter space and (2) providing instantaneous all-sky electromagnetic coverage and prompt localization of gravitational wave sources. These goals led to the development of a strawman concept for a future mission known as the Advanced Particle-astrophysics Telescope (APT). While the APT design is optimized for γ-ray performance, the instrument would also provide key CR measurements that address the same scientific questions: (1) The MeV–TeV γ-ray measurements would provide an order of magnitude improvement in DM upper limits from stacked Dwarf galaxy observations compared with Fermi; at the same time, very high energy measurements of the Boron to Carbon ratio could provide key constraints on CR propagation models essential for using positron and antiproton data to look for a DM signal. (2) The excellent sensitivity, large instantaneous field of view (fov), and sub-degree point source localization of APT in the MeV range (from Compton imaging) will provide efficient alerts for multimessenger follow-ups of gravitational wave sources and short GRBs. At the same time APT will provide measurements of the elemental abundances of ultra-heavy elements in the galactic CRs, providing a key method to distinguish between a supernova or neutron-star origin for r-process elements.

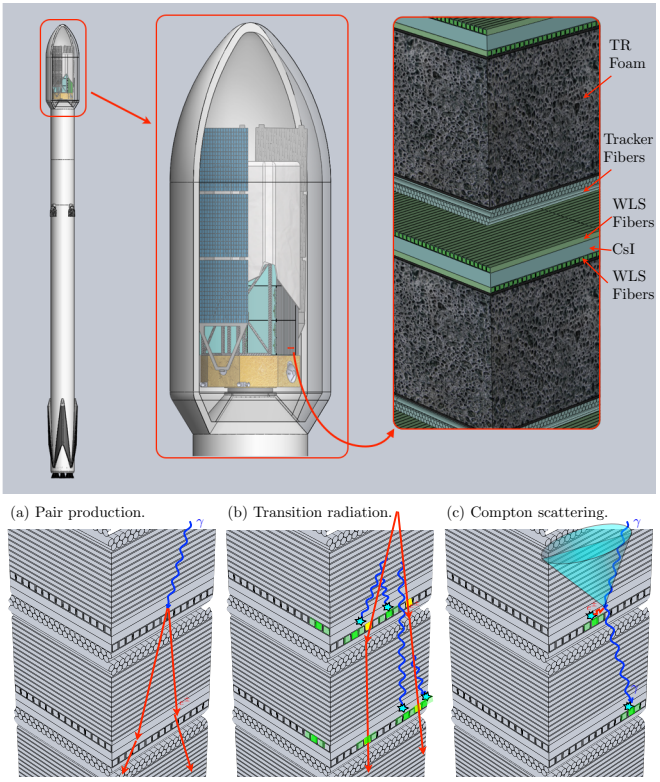

Figure 1: *Top: APT in Falcon-9 faring. Bottom: APT detection modes.*

The most challenging requirement to achieve these scientific goals is the need to dramatically increase the effective area and instantaneous *fov* of a future instrument without increasing the cost of the mission compared with current generation experiments like *Fermi*. The APT mission concept began as a probe-class γ-ray experiment (See the NASA Physics of the Cosmos Program Analysis Group whitepapers). Subsequently we descoped the mission concept to fit in a small or MIDEX-sized experiment budget envelope. The cost and mass constraints motivate the development of alternatives to Si-strip detectors and deep electromagnetic calorimeters used in similar instrument designs; while these can achieve excellent position or energy resolution (essential for some science programs) there is no practical way to scale these to meet the requirements for DM and transient science. Here we propose using very long scintillating fibers read-out by modern solid-state photodetectors (SiPM) around the perimeter of a large detector volume. The detector volume is a simple stack-up of scintillator (plastic and CsI crystals) with no need for internal electrical connections and no dead space between detector elements. Unlike Si detectors, the channel count scales with the surface area rather than detector volume, and challenging noise problems are mitigated by using detector devices with avalanche gain.

Laboratory tests of small prototypes of the SOFT and ICC detectors coupled with simulations demonstrate that most of the requirements for Compton and pair imaging can be met. Accelerator beam tests of a larger scale prototype that vertically integrates all of the detector components

are underway. In parallel with these measurements, a piggy-back balloon instrument is being constructed for an Antarctic balloon flight this year. Together, these measurements should advance the technical readiness level of the concept, allowing formulation of a detailed proposal in a three year time-scale.

If the different detection modes (multiple-Compton scattering, pair tracking, transition radiation, and multiple differential ionization energy loss dE/dx for heavy ions - see Fig. 1) can be demonstrated, given the scalable detector design, we can confidently extrapolate performance to a large volume detector. Coupled with the good heritage of scintillating fibers in space, this should result in a simple detector design with minimal technical risk but very high scientific impact in astroparticle physics.

2 Scientific Objectives

Analysis of *Fermi* LAT data on Milky-Way satellite dwarf galaxies has resulted in some of the most powerful constraints on models of WIMP dark matter up to >100 GeV masses [6] and underscores the important role of indirect detection on solving the dark matter problem. With more than an order of magnitude improvement in exposure factor in the GeV range and with extended coverage of the continuum spectrum down to MeV energies, APT would be in a position to detect or rule out the entire natural parameter space for a thermal WIMP up to TeV mass scales (see Fig.2). Observational capabilities in the MeV would enable both multiwavelength searches for the inverse-Compton counterpart to emission from massive DM candidates, and the search for sub-GeV candidates, which remain largely unexplored to-date. The recent discovery of gravitational waves (GWs) from a neutron-star merger by the LIGO collaboration [2] points to the potential for GW experiments and the importance of all-sky instruments for multi-wavelength/multi-messenger astronomy. These n-star mergers, like short γ-ray burst (GRB) sources, are difficult to study given the lag in re-pointing narrow-field instruments. Instantaneous all-sky coverage is key to detection and localization of these events; the γ-ray band is one of the few wavebands (over the entire electromagnetic spectrum) in which such coverage is possible. The very large effective area of APT in the MeV to multi-GeV regime would be ideal for detecting emission from short GRBs and GW sources. For GRBs, the *Fermi* LAT has only detected the brightest events near the high end of the fluence distribution; thus an improvement in effective area is as important as the larger instantaneous FoV.

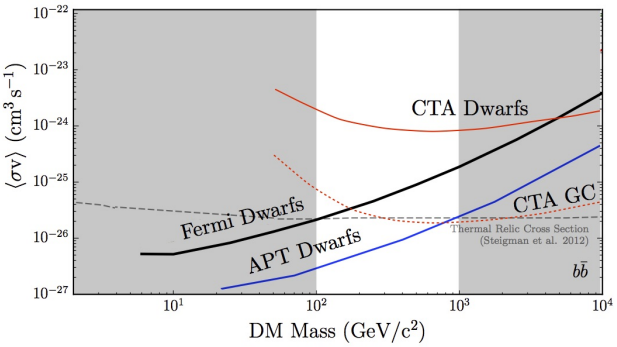

Figure 2: *Estimated sensitivity of APT to DM.*

APT makes use of multiple layers of long scintillating fibers and thin Sodium-doped CsI (CsI:Na) tiles covering an area of 3m×3m. With a thickness of $<\sim$ 6 radiation lengths (r.l.), APT trades energy resolution for a very large effective area and *fov*. By replacing the passive converter layers (e.g., the tungsten foils employed in *Fermi*) with imaging CsI detectors, the instrument will function both as a pair telescope for 60 MeV to $\sim$ 1 TeV γ-rays and as a Compton telescope with excellent sensitivity down to $\sim$300 keV. Thus, in addition to constraining the most compelling WIMP models, the excellent energy resolution for low energy pair events would make it possible to resolve spectral features from light MeV to GeV dark matter (e.g., from meson intermediate states). The very large area Compton telescope would extend energy coverage down to lower energy continuum emission and/or lighter MeV dark matter.

At >10 GeV energies, where effective area rather than background begins to become the dominant factor determining sensitivity, the much larger instrument would result in an order

of magnitude improvement in *sensitivity* compared with *Fermi*. While the Compton angular resolution would be somewhat limited compared to semiconductor-based Compton telescopes, the enormous effective area and high detection efficiency would result in an improvement in sensitivity in the ∼0.3 MeV to 20 MeV regime by orders of magnitude compared to any extant instrument. In the Compton regime, the higher detection statistics would more than compensate for the slightly reduced resolution for localization and spectral measurements of transient sources (see Fig. 3). The novel up-down symmetry of the instrument (and Lagrange-point orbit) would allow particles to enter from the top or bottom of the instrument, providing close to a 4π-sr field of view, making this a uniquely capable instrument for multi-messenger observations of astrophysical transients.

Another unique feature of the instrument concept is incorporation of transition radiation (TR) detectors by using foam materials (with numerous interfaces) for the composite support structure between the CsI planes. Preliminary calculations and past studies indicate that with the use of high-energy TR detectors (with thick TR converter layers and CsI detectors for >100 keV X-rays) could potentially provide energy measurements of light CR nuclei up to 50 TeV/nucleon [13, 41]. The capability of APT to measure the high energy spectrum of light CRs also has a bearing on the primary DM science driver. A number of CR experiments show evidence for a rising positron fraction at GeV energies [4, 5, 7]. This observation is difficult to explain from standard models for CR propagation [28]. The solution to these problems could come in the form of new models for CR propagation and secondary production [15, 25], could point to contributions from local pulsars [20], but might also point to new physics (e.g., leptophillic dark matter or a nearby DM density enhancement [14]). Using TR detection, the instrument would provide measurements of CRs with energies approaching the knee in the all-particle spectrum (Fig. **??**). In particular, this capability could result in the measurement of the secondary to primary ratio of CRs up to ∼tens of TeV energies. High statistics measurements of the B/C ratio at energies > 3 TeV/nucleon (i.e., Lorentz $\gamma > 3000$) are key to distinguishing between different scenarios for CR propagation and secondary positron production [15, 25]. APT, with its geometry factor ∼30 m^{2}sr (an order of magnitude larger than that of the proposed ISS-CREAM instrument or AMS-02) and TR measurements up to $\gamma \sim 10^5$ would provide definitive data to distinguish between these various scenarios.

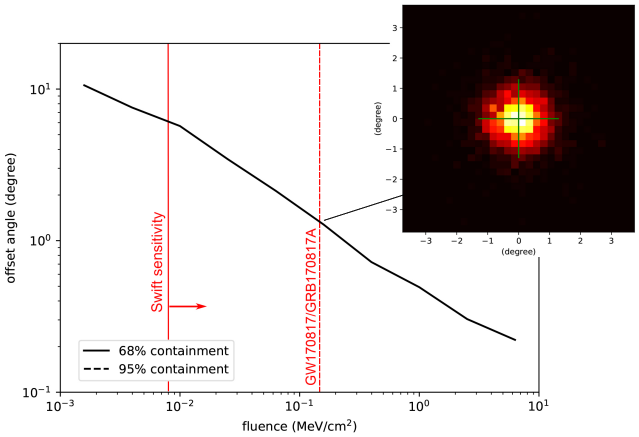

Figure 3: *Compton event localization error versus fluence. Inset shows simulation corresponding to the GW170817 event.*

APT would provide other CR measurements that complement the MeV gamma-ray detections of n-star mergers. For many years it has been thought that ultra-heavy ($Z > 30$) r-process nuclei were synthesized in core-collapse supernovae (CCSNe). However, in recent years there have been a flood of papers suggesting that a large fraction, or even all, of r-process nuclei are synthesized instead in binary neutron star mergers (BNSM) [17, 22–24, 31, 42–44]. Current supernova models are not able to produce the abundances of r-process ultra-heavy nuclei in the second ($Z = 51 - 55$) and third ($Z = 75 - 79$) r-process peaks that are consistent with solar system abundances [21, 39, 44]. Additionally, observations of metal-poor stars in the galactic halo of the Milky Way show that r-process abundances in the second and third r-process peaks are consistent with solar system abundances. This requires a second source of r-process nuclei in

addition to CCSNe [42]. Although CCSNe are $\sim$ 1000 times more frequent than BNSM in the Milky Way, the amount of r-process material ejected in a BNSM is much larger than for CCSNe [23]. Measurements of r-process nuclear abundances in CRs provide a unique method, based on measurement of the abundances of the actinides (Th, U, Pu, and Cm), of testing whether CCSNe or BNSM are responsible for the heaviest r-process nuclei in the contemporary cosmic rays. If the source of the actinide nuclei is CCSN, $_{94}$Pu (half-life 81 Myr) and $_{96}$Cm (half-life 16 Myr) should be present in the early solar system abundances relative to $_{90}$Th since they would not have decayed. On the other hand, if BNSMs with lifetimes 100 Myr [22] are the source of these nuclei, then $_{96}$Cm should be essentially completely decayed and $_{94}$Pu should be partially decayed (Fig. **??**). In addition, measurements of the r-process groups $Z = 51 - 55$, $Z = 62 - 69$, $Z = 76 - 78$ as well as $Z = 34 - 37$ (which are roughly half produced by the r-process [29]) can be used to distinguish between the various models of r-process production by BNSMs. APT measurements of elemental abundances through measurements of dE/dx versus total E could provide an increase in statistics on ultra-heavy abundances orders of magnitude above the sensitivity of current experiments.

3 Technical Description of the APT Mission

The straw-man APT instrument module has a cross-sectional area of 3m×3m and a height of 2.5m, consisting of 20 $x - y$ tracker and calorimeter layers (Fig. 1) A probe-class instrument would include 2 such modules, but we focus the discussion (and simulation results) on a single 3m-square instrument. The tracker layers are formed from 2 close-packed, staggered layers of 1.5mm diameter round scintillating fibers, aligned by a comb-like structure. Close-packing the fibers allows improved position resolution (from centroiding pulse heights from overlapping layers) and very high detection efficiency. In place of passive pair converter layers 20 layers of CsI:Na detectors are interleaved between the tracker layers. Green (or red/green) wavelength shifting (WLS) fibers (2mm square) covering thin (∼5mm) CsI tiles are used to collect and shift the UV/blue emission from the CsI:Na and pipe a fraction of the isotropically re-emitted light to the SiPMs. Fibers are bonded to the tiles using a UV transparent silicone or epoxy that also acts to hermetically seal the mildly hygroscopic scintillator. For better light collection, WLS fibers on the CsI can be split into two 1.5m long fibers with a mirrored central surface, and a 3mm SiPM at each end. The addition of a second layer of red fibers reclaims some of the escaping green light, piping it to the same SiPM for the green layer. Laboratory attenuation length measurements (included in our GEANT simulations) have yielded attenuation lengths of >1.0 m for both green and red-green fibers. Centroiding the light collected by the orthogonal WLS fibers bonded to either side of the CsI crystals provides the $x - y$ coordinates of the interaction (see Fig. 4). The use of long scintillating fibers read out at the edges of the instrument with SiPMs allows the very large passive volume to be read-out by a total of 380,000 channels, less than half that for the *Fermi* instrument (∼800,000). This approach also allows for higher tracker conversion efficiency and imaging calorimetry. The design has no gaps or embedded electronics in the detector volume,

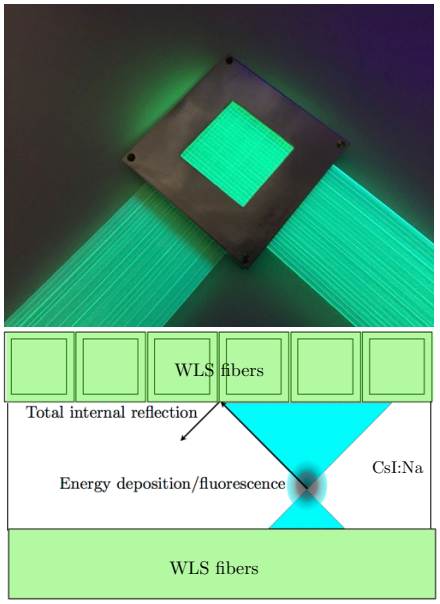

Figure 4: *Top: First prototype CsI/WLS fiber detector. Bottom: Illustration of $x-y$ imaging with WLS fibers. A similar setup with a single 50mm CsI tile was used for the CERN beam test but with a modified version of the VERITAS 500 Msps FADC electronics.*

dramatically simplifying the distribution of signals and power.

A composite structure (doubling as the TR radiator) supports the weight of each plane allowing each to be handled as a stand-alone module. The support structure consists of two 0.7mm carbon fiber plates sandwiching a 5cm thick foam core. A single layer of CsI with a mass of 203 kg would result in $\sim 300\mu$m deflections at the center of a 3m detector plane. An external space frame rigidly bolts to inserts in each composite layer, and provides the mounting points for the electronics and the anticoincidence detector (ACD). The ACD would likely consist of tiles of 1m×1m by 1cm thick plastic scintillator with embedded 2mm square WLS fiber (the presence of the ACD material is included in all simulations). The ACD is segmented and read out by programmable logic to allow one to identify γ-ray or CR events, without vetoing γ-ray events when the electromagnetic shower extends beyond the detector volume. Fibers spaced every 1-2 cm placed in groves will be merged into a set of SiPMs and readout electronics identical to that used for the tracker. Two 3m-square modules fit in the faring of a Falcon 9 rocket (Fig. 1).

The APT readout electronics would consist of front-end ASICs (including preamplifiers, comparators with programmable thresholds, and SiPM bias voltage control) followed by analog-pipeline waveform digitizing ASICs. These ASICs closely follow on past designs of the T5TEA trigger ASIC and the TARGET C ASIC designed by Co-I Varner, and used in our prototype electronics [8, 10, 18, 26, 34, 40]. The SiPMs have high gain ($\sim 10^6$) and high quantum efficiency ($\sim$50%) alleviating the need for very low-noise electronics. The readout electronics design is somewhat challenging due to the combination of fast signals from the plastic scintillating fibers combined with the relatively long decay time of the CsI:Na fluorescence signals. The dynamic range requirements for detecting both minimum-ionizing particles (MIPs) and high-Z nuclei are also a challenge. However, the long timescale of the CsI fluorescence and very high level of oversampling of the slow CsI signal has been shown to dramatically extend dynamic range. The analog pipeline ASICs store charge on a series of analog memory cells (capacitors) controlled by a high speed clock that sequentially connects the input signal to the capacitors and forms a continuously overwritten analog ring buffer. After a trigger, a region of interest in the analog buffer is addressed and digitized using a number of simple Wilkinson run-down ADCs. These devices can realize very low power operation since, only after a trigger signal arrives is the analog to digital conversion started (bias currents on comparators are only turned on when required for acquisition). With NASA APRA funding we are redesigning the existing TARGET ASICs to use lower sampling speeds ($\sim$100 Msps) and lower power with a realistic design goal of $<$5 mW/ channel.

The front-end ASICs will come in two variants, one for the fast, small dynamic range signals from SOFT detector or ACD system, and one for the CsI/WLS (ICC) fiber signals. The analog sum and comparator design would be based on the TARGET 7 and T5TEA designs [8, 10, 18, 26, 34, 40]. Using techniques developed for the SiREAD ASIC, DACs inside these ASICs would provide bias voltages to the SiPMs. We anticipate that all high-level triggers will be formed by sending serial hit data to FPGAs. A pair-event trigger (PET) would be formed from a coincidence of hits in the tracker fibers in a single $x-y$ plane, coincident with a hit in an adjacent plane. With a minimum expected signal of 15 p.e., a 4 p.e. threshold would provide 99.91% detection efficiency in a single 1.5mm fiber. The same threshold would give a single fiber dark trigger rate of 0.56 Hz if one assumes an 89 kHz dark count rate for a 2mm square SiPM passively cooled to 5°C and a 5% afterpulse/crosstalk fraction for the SiPM. For a simple trigger formed by a coincidence in any of the 20 $x-y$ planes, the rate would be 3 Hz for a 40 nsec coincidence window. A Compton-event trigger (CET) would be formed by first summing the signal from 8 adjacent fibers then sending this to a comparator to form the Level-0-CET trigger (similar to the T5TEA design). The CET would require coincidences between the L0

signals from corresponding x and y plane forming the L1-CET trigger. A further coincidence of multiple planes would form the final CET. Assuming a threshold of 6 p.e. in the summed signal from each group of fibers (L0) and a coincidence time of 5μsec, one obtains an accidental coincidence rate of 0.11 Hz. Thus, to a good approximation, raw trigger rates are dominated by CR background events. We calculate a raw average CR trigger rate of 350 kHz (660 kHz) for a 51 deg low-Earth orbit at solar max (solar min) and 950 kHz (1900 kHz) for an L1 orbit at solar max (minimum). The ACD together with the other detector data would be analyzed to identify the relatively low rate of high-Z CR events, forming a third Cosmic-Ray Trigger (CRT). Following either a CET, PET or CRT trigger, buffered signals from tracker and WLS channels would be read out by GHz serial links to the DAQ FPGAs. Buffered events would then be sent to the telemetry system using real-time pipelined FPGA-based processing to select good events from the topology of tracker, CsI and ACD hits. An analog pipeline with 5 μsec depth (500 cells) would be sufficient to provide enough trigger latency to postpone integration and digitization until after the formation of the delayed CET, dramatically reducing power consumption and simplifying event buffering.

Scintillating fibers have been used successfully on numerous experiments flown on satellites and high-altitude balloons following their development in the 1980s [12, 16] In space, WU fibers have been used as a hodoscope and trigger on the Cosmic Ray Isotope Spectrometer (CRIS) launched on the NASA Advanced Composition Explorer (ACE) spacecraft in 1997 [33]. After more than 20 years in space, the instrument continues to acquire excellent data for the detection of nuclei with charge $Z \geq 3$. WU fibers are being used on the *Fermi* γ-ray telescope as part of the anti-coincidence detector [9]. Most recently, the Calorimetric Electron Telescope (CALET) (launched to the International Space Station (ISS) August 2015) CALET uses scintillating fibers for the imaging calorimeter that tracks particles (electrons, protons, and nuclei) and serves as the front end (first 3 radiation lengths) of the calorimeter [36, 37]. On high-altitude balloons, scintillating fibers have been used on several detectors. The Trans-Iron Galactic Element Recorder (TIGER) instrument which detected heavy and ultra-heavy CRs, used fibers for the hodoscope [30] for two flights over Antarctica. Its successor, the SuperTIGER experiment, which flew on a record long 55-day balloon flight over Antarctica in 2012-2013, also used scintillating fibers for the very large hodoscope. This was a very large hodoscope which had dimensions for each plane of 1.15 m$\times$2.4 m produced in the WU fiber lab by Binns [11]. Calculations performed using the SPENVIS program indicate that for a 10 year mission in a 550km, 28.5 degree inclination orbit, the dose in space is <1kRad near the edge of the detector, assuming a shielding of 1.25 cm Aluminum equivalent. Radiation damage studies on blue-emitting fibers indicate that we should not expect significant damage for that level of radiation [1, 35]. Valls et al. [38] found a small degradation in green emitting fibers in radiation damage studies for this dose level. So it is possible that over a 10 year period there might be small signal shifts, but they would be easy to compensate for using in-flight calibration. The Valls et al. result should be considered a worst case since the dose in space is accumulated over a long period of time, allowing the scintillator to recover spontaneously as free radicals recombine.

Simulations of this baseline APT design were performed in Geant4 using measured performance parameters from prototype tracker fibers and a prototype of the CsI detector (see Fig.5) Geant4 is used to calculate energy deposition in the various detectors including full particle and γ-ray interactions. To speed simulations, we use simple approximations for the optics including results of laboratory measurements for light output from scintillating fibers in response to singly charged minimum ionizing particles (MIPs) and the measured light output of WLS fibers on our CsI detector prototypes (see Fig.6). The 5mm CsI layers result in a total thickness of 5.4 radiation lengths of active CsI.

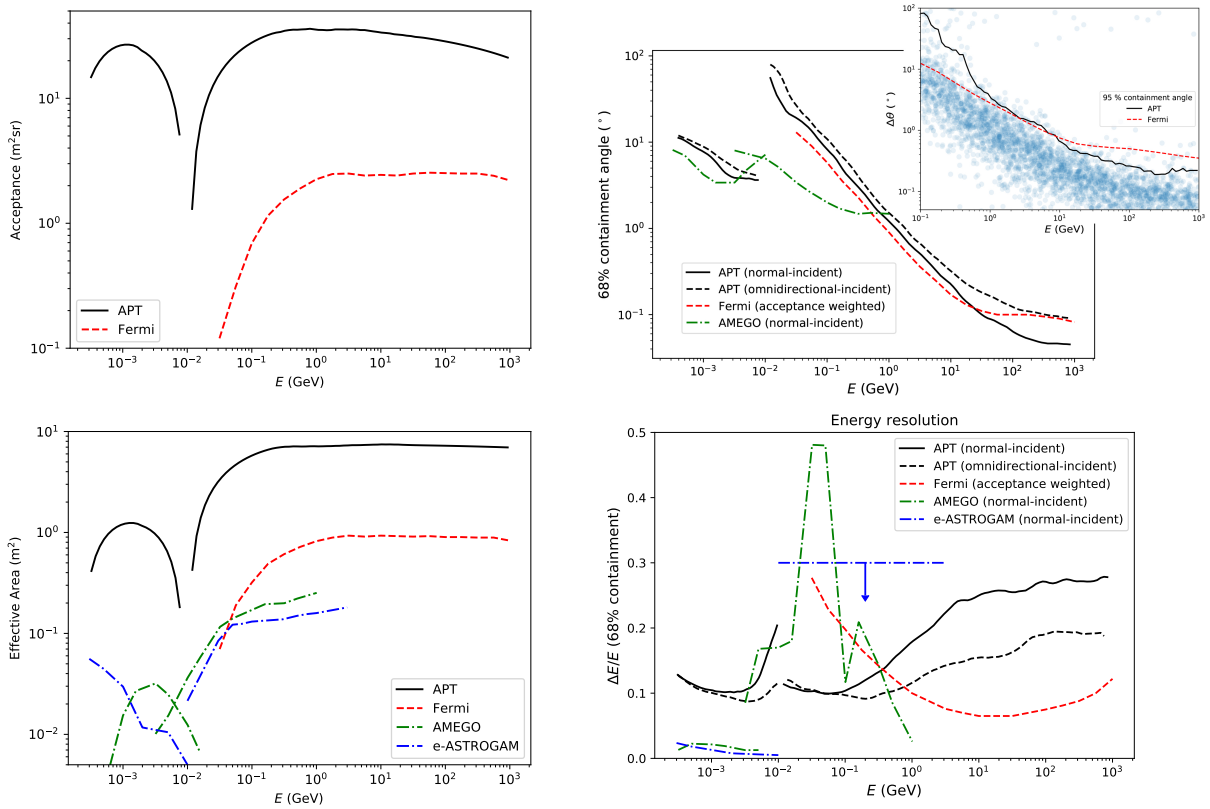

Figure 5: *(a) Acceptance/geometry factor and (b) normal-incident effective area vs. energy. (c) Angular resolution with inset scatter plot of individual event reconstruction errors. (d) Energy resolution comparison. The solid black curves denote APT Compton and Pair reconstruction for the 3m×3m MIDEX concept. Dashed red, dash-dotted green, and dash-dotted blue curves are for Fermi P8R2_SOURCE_V6 events, AMEGO, and e-ASTROGAM, respectively.*

The foam layers between CsI detectors provide numerous interfaces for the production of transition radiation. To bracket the possible configurations, we simulated an instrument with Al foam and dielectric foam radiators in 3 varieties: (1) Al foam with 80 layers of 0.05mm Al + 0.6mm gaps, Al foam with 14 layers of 0.5mm thickness and 2mm gap and Mylar foam with 100 layers 0.02mm thickness and 0.4mm gaps). Even with the thicker Al foam material, simulation results of the angular resolution for pair events are comparable to *Fermi* Pass-8 source-class events, and Compton resolution for individual events is negligible (although the effective area is reduced).

From the scatter plot in the inset of left Fig. 5, it is likely that we will be able to apply data quality cuts to identify events with substantially better angular resolution than *Fermi* (similar to the front events for the *Fermi* instrument). Given the large increase in effective area, APT would also provide many more high-energy events than *Fermi* and thus have a substantially better resolution depending for typical source spectra.

We note that all of our simulated performance plots use the same set of fully reconstructed events (not, e.g., a subset of events with the best resolution). We also note that we include radiator material in all simulations (Compton angular reconstruction), and use conservative estimates for light collection efficiency based on laboratory measurements.

CsI:Na has a scintillation light spectrum that peaks in the blue at around 420nm. Fibers using green K-27 WLS dye can efficiently absorb 420nm CsI:Na scintillation light, isotropically re-emitting green light of which about 4% is collected at each end of the fiber. By using crossed

2mm fiber planes (one in the x-direction on top and one in the y-direction on the bottom of the crystals) and a UV-transparent silicone to bond the crystals to the fibers, one achieves sufficient light collection. Fibers formed of two layers of green and red WLS (in a single 2mm square fiber) have been fabricated at WU and were used in the CERN beam test. The red fiber layer can almost double the light collection efficiency, reclaiming some of the large fraction of light that escapes the green WLS region (this improvement is not included in our simulation studies). The acceptance cone corresponding to the total internal reflection angle subtends a number of fibers, allowing one to centroid the interaction point in the CsI.

The Compton angular reconstruction depends on the energy resolution and hence on light collection efficiency. The principal limitation of using thin CsI comes from the error in this angle produced by the finite energy resolution. As energies increase, the probability for multiple Compton scatters increases and analysis becomes complicated by ambiguities in identifying the order of scatters. For the simulation study we use an algorithm where we consider every possible ordering up to 10 scatters and demand consistency in positions and corresponding energy deposition. Energy is reconstructed using the total signal measured in the CsI detectors. To construct a 2-D PSF, one needs to combine the ring-like regions (with radius corresponding to the Compton angle) for each event. For our simulation study, we used a simple algorithm where one uses the minimum distance to the ring for each event. To determine the error in the resulting source position, we assumed a source location and fluence with a typical GRB Band spectrum, then ran multiple trials where we reconstructed the source position; using this method we derived an explicit Monte-Carlo calculation of the reconstructed source location error (Fig. 3). The on-axis effective area for Compton imaging peaks at $\sim$1m^2 (200 times larger than that of COMPTEL effective area [32] and 30 times larger than the geometric area of the proposed AMEGO instrument [27]). While future missions like AMEGO should offer reduced backgrounds and improved energy resolution especially important for studying galactic sources, for transients like short GRBs backgrounds should be negligible. The effective area and *fov* are the most important attributes for transient sources like γ-ray bursts, where sensitivity should scale almost directly with area and the number of detected sources should scale directly with solid angle. In Fig. 3 we show the sensitivity of GRBs of varying fluences (measured in the 0.3-10 MeV band) for a typical burst spectrum. Given the relatively flat νF_ν spectrum, this fluence is comparable to that measured in the Swift band. Sensitivity would extend to much lower fluences than detectable with Swift (10^{-8}erg cm^{-2} in the 15-150 keV band) perhaps revealing new, as yet undiscovered, source populations. Also shown is a simulation of the n-star merger event GW170817/GRB170817A, using the estimated spectrum [3, 19]. For this event, even using our very simple algorithm for point source localization (see inset) APT would provide a positional uncertainty of $\approx 1^\circ$ much better than $\sim 15^\circ$ GBM error circle.

Following this simulation study, additional work was done to develop new high-speed algorithms for sequencing multiple scatters and producing a weighted reconstruction of arrival directions. Using optimized algorithms we can reconstruct 50,000 events (giving arrival direction and energy of each photon) in 1 second on a quad-core 1.4GHz Arm Cortex processor. Binning weighted rings on a tesselated 10k-vertex sphere allows combining these event to localize a source to better than a degree in less than 1 second. Remarkably, a single flight computer (similar to a Raspberry Pi) can provide a source localization within 1 second for prompt notifications to ground stations and to the multi-messenger community.

For ultra-heavy CRs, the CsI detectors in APT provide measurements of the energy deposition ΔE of an incident particle in each detector layer of r.l. Δx. The so-called $dE/dx - E$ technique can be used to identify the charge and mass of energetic nuclei of the incident particle. Neglecting saturation effects, the light yield in the first layers is proportional to Z^2. The results of our

Geant4 simulations show good separation of elements up to a $Z \sim 92$ with a supervised machine learning algorithm used to correct for energy losses in passive materials. Results of a CERN heavy ion beam test of one APT CsI detector layer confirm these simulation results, and further indicate that saturation effects (up to Pb nuclei) are minimal in the CsI detector.

4 R&D Work

A funded NASA APRA grant supports construction of a working prototype of a 4-layer instrument that integrates all of the components of APT including a scintillating fiber tracker, CsI crystals readout by WLS fibers and SiPMs using prototype electronics incorporating TARGET ASICs of a similar design to those required for a flight instrument, the redesign of a lower power readout ASICs, and accelerator tests of the prototype detectors. Recently, we were also approved to fly a piggy-back instrument testing a single 150mm square CsI detector and 120 channels of TARGET readout electronics on a long-duration balloon flight (the SuperTiger CR instrument). Triggers coincident with SuperTiger will provide additional data on detector response to CR (Fe-group) nuclei, as well as providing data on upward going MeV gamma-rays from atmospheric interactions.

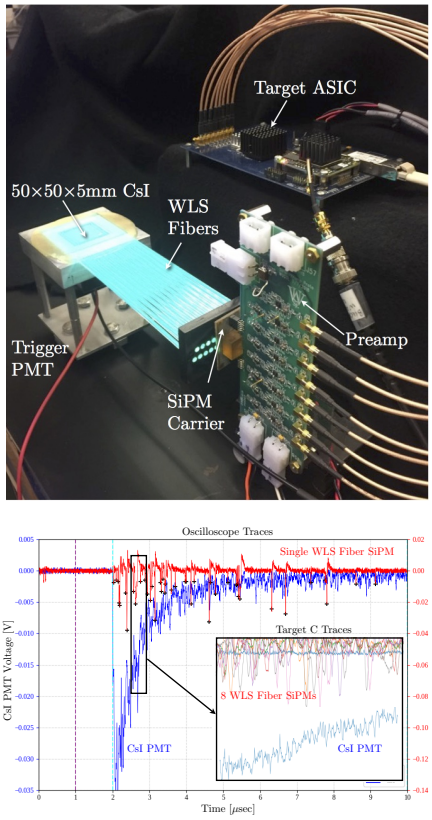

Figure 6: *Top: Prototype CsI detector, preamp and TARGET ASIC board. Bottom: Traces captured with oscilloscope from a single SiPM, and with the TARGET ASIC from all 8 SiPMs but limited to a 512 nsec window (single p.e. pulses are clearly visible in both traces). The data are consistent with ≈240 p.e. per 662 keV in one WLS fiber plane.*

A number of laboratory measurements have already been made to test the detector elements. Detection efficiency and attenuation length measurements have been made for both the tracker fibers (in response to ^{90}Sr electrons) and wavelength-shifting fibers (in response to a pulsed LED). A first simple prototype CsI detector consisting of a single plane of Saint-Gobain WLS fibers bonded to the top of a 5mm thick 50mm square CsI:Na tile was used to determine parameters for simulations. A PMT bonded directly to the bottom of the CsI tile provided a reference trigger. We tested the device using a collimated 17 mCi Cs-137 source with a 662 keV X-ray line. The summed output from 8 WLS fibers was read-out with a Hamamatsu 1390 PMT. Correcting for the difference in QE of the R1398 (15% averaged over the WLS output spectrum) and the Hamamatsu SiPMs planned for use in the beam-test instrument we derived a light output of 128 p.e from a single CsI layer for the total absorption of a 662 keV X-ray. Simulations of an identical prototype geometry were used to calibrate the light collection efficiency.

We retested the prototype detector with an array of 8 3mm Hamamatsu S14160-3050 SiPMs on a carrier board, with a custom 8-channel preamplifier board (Fig. 6). Signals from the 8 preamplifier outputs were readout by a TARGET C (TC) evaluation board produced (designed by the UE group). The TC evaluation board incorporates the TARGET C ASIC (developed by Co-I Varner) as well as a custom trigger ASIC (T5TEA), a control FPGA and Gbit fiber-optic data interface to a data acquisition computer. (These boards were recently modified to instrument 32 channels and fit in a 4U form-factor for the beam test instrument.) Data was with the Cs-137 source and using the R7600 to provide the external trigger for the TC board.

Fig. 6 shows a typical event where one can count single p.e.s (the fast dips in the SiPM signals).

For a CERN HI beam test, we used a similar setup with a revised preamp design, and covering 30 fibers with SiPMs and readout electronics. To cover the additional channels, we used a revised version of the 8bit 500 Msps FADC boards developed by the WU group for the VERITAS experiment. Even with limited dynamic range, we were able to reconstruct the charge of the heaviest ions (Pb) in the CERN beam, but using the (unsaturated) tail of the pulse. A similar technique will be used to extend the dynamic range using the TARGET ASICs.

5 Budget and Schedule

At a JPL A-team review in May 2015, we verified that for a simple extrapolation of the *Fermi* detector to a 7 r.l. 3m×6m APT concept, the instrument weight and volume was compatible with a Dragon 9 launch to LEO Fig. 1 and the total cost could plausibly fit in the ∼1G$ probe-class mission. As part of this study, we determined that an acceptable radiation exposure could be obtained in either a low Earth orbit, or a Sun-Earth L1 or L2 orbit for a 10 year mission life.

Subsequently, we revised the design to employ a shallower calorimeter and reduced the detector active area by half. While we have not conducted another NASA costing exercise, we used a conservative grass-roots cost estimate using (quoted) small quantity costs of tracker and calorimeter fibers as well as 150mm×150mm×5mm tiles. All detectors (including the Tracker, WLS fibers and ACD tiles) use essentially the same SiPM photodetectors, preamp ASICs and digitizer electronics, simplifying the enginneering design. We include 15 FTE years for engineers and 20 FTE years for technicians. This results in a total scientific payload cost of 50M$ for the instrument.

The largest cost uncertainty comes from the launch vehicle and payload mass. For a mass estimate we use the density of CsI and polystyrene to calculate the active detector mass. To this we add the mass of the foam/carbon fiber support panels needed to make each detector plane self supporting, as discussed above. We include a very rough estimate for the mechanical support structure, the spacecraft bus and solar panels. Rough estimates of the weight of the anticoincidence system, electronics, and micro-meteorite shield are also included to obtain a payload mass of 8000-9000 kg.

The spacecraft requires no active repointing but must be able to determine absolute pointing to <0.5 arcmin, maintain attitude for solar panels and passive radiators (for electronics cooling) and must be able to maintain an L1 orbit for up to 10 years. Solar panels should provide 5-10kW of power. The biggest uncertainty of the cost comes from the launch vehicle needed to lift such a heavy instrument into a high orbit. Space-X has successfully launched two Falcon 9 Heavy launch vehicles, improving the chances that such a large instrument could be lifted to a low Earth orbit. The advertised lift capacity of the Falcon Heavy should be sufficient to lift a 9000 kg into a high orbit, but the details of such a launch (e.g., effect of partial recovery of boosters on cost, or methods of achieving a Lagrange orbit) have not been determined. Descope options include reduction in the depth of the calorimeter (reducing the maximum energy reach), or launch to a low-Earth orbit (resulting in a factor of 2 reduction in total field of view and hence exposure).

After completing our three-year RD study (Oct 2018 to Sept 2021) we will apply for one-year funding to complete a design study. During this period we hope to finalize the design of the readout electronics, support structure, and to complete specifications of the spacecraft design. At this point, a proposal will be developed for a MIDEX or Probe opportunity. Delivery of fibers and CsI would take approximately 3 years. Integration of the instrument should be relatively straightforward, given the small number of detector subsystems, in-flight calibration, and modularity of the design.

References

References

[1] Abbott; et al. " ," In *IEEE Trans. NS*, v. 40, 1993, p. 476

[2] Abbott, BP; Abbott, R; Abbott, TD; Abernathy, MR; Acernese, F; Ackley, K; Adams, C; Adams, T; Addesso, P; Adhikari, RX; et al. "Observation of Gravitational Waves from a Binary Black Hole Merger," *Physical Review Letters*, v. 116(6), 2016, p. 061102. `http://adsabs.harvard.edu/abs/2016PhRvL.116f1102A`

[3] Abbott, BP; et al. "Gw170817: Observation of gravitational waves from a binary neutron star inspiral," *Phys. Rev. Lett.*, v. 119, 2017, p. 161101

[4] Accardo, L; Aguilar, M; Aisa, D; Alvino, A; Ambrosi, G; Andeen, K; Arruda, L; Attig, N; Azzarello, P; Bachlechner, A; et al. "High Statistics Measurement of the Positron Fraction in Primary Cosmic Rays of 0.5-500 GeV with the Alpha Magnetic Spectrometer on the International Space Station," *Physical Review Letters*, v. 113(12), 2014, p. 121101. `http://adsabs.harvard.edu/abs/2014PhRvL.113l1101A`

[5] Ackermann, M; Ajello, M; Allafort, A; Atwood, WB; Baldini, L; Barbiellini, G; Bastieri, D; Bechtol, K; Bellazzini, R; Berenji, B; Blandford, RD; Bloom, ED; Bonamente, E; Borgland, AW; Bouvier, A; Bregeon, J; Brigida, M; Bruel, P; Buehler, R; Buson, S; Caliandro, GA; Cameron, RA; Caraveo, PA; Casandjian, JM; Cecchi, C; Charles, E; Chekhtman, A; Cheung, CC; Chiang, J; Ciprini, S; Claus, R; Cohen-Tanugi, J; Conrad, J; Cutini, S; de Angelis, A; de Palma, F; Dermer, CD; Digel, SW; Do Couto E Silva, E; Drell, PS; Drlica-Wagner, A; Favuzzi, C; Fegan, SJ; Ferrara, EC; Focke, WB; Fortin, P; Fukazawa, Y; Funk, S; Fusco, P; Gargano, F; Gasparrini, D; Germani, S; Giglietto, N; Giommi, P; Giordano, F; Giroletti, M; Glanzman, T; Godfrey, G; Grenier, IA; Grove, JE; Guiriec, S; Gustafsson, M; Hadasch, D; Harding, AK; Hayashida, M; Hughes, RE; Jóhannesson, G; Johnson, AS; Kamae, T; Katagiri, H; Kataoka, J; Knödlseder, J; Kuss, M; Lande, J; Latronico, L; Lemoine-Goumard, M; Llena Garde, M; Longo, F; Loparco, F; Lovellette, MN; Lubrano, P; Madejski, GM; Mazziotta, MN; McEnery, JE; Michelson, PF; Mitthumsiri, W; Mizuno, T; Moiseev, AA; Monte, C; Monzani, ME; Morselli, A; Moskalenko, IV; Murgia, S; Nakamori, T; Nolan, PL; Norris, JP; Nuss, E; Ohno, M; Ohsugi, T; Okumura, A; Omodei, N; Orlando, E; Ormes, JF; Ozaki, M; Paneque, D; Parent, D; Pesce-Rollins, M; Pierbattista, M; Piron, F; Pivato, G; Porter, TA; Rainò, S; Rando, R; Razzano, M; Razzaque, S; Reimer, A; Reimer, O; Reposeur, T; Ritz, S; Romani, RW; Roth, M; Sadrozinski, HFW; Sbarra, C; Schalk, TL; Sgrò, C; Siskind, EJ; Spandre, G; Spinelli, P; Strong, AW; Takahashi, H; Takahashi, T; Tanaka, T; Thayer, JG; Thayer, JB; Tibaldo, L; Tinivella, M; Torres, DF; Tosti, G; Troja, E; Uchiyama, Y; Usher, TL; Vandenbroucke, J; Vasileiou, V; Vianello, G; Vitale, V; Waite, AP; Winer, BL; Wood, KS; Wood, M; Yang, Z; Zimmer, S. "Measurement of Separate Cosmic-Ray Electron and Positron Spectra with the Fermi Large Area Telescope," *Physical Review Letters*, v. 108(1), 2012, p. 011103. `http://adsabs.harvard.edu/abs/2012PhRvL.108a1103A`

[6] Ackermann, M; Albert, A; Anderson, B; Atwood, WB; Baldini, L; Barbiellini, G; Bastieri, D; Bechtol, K; Bellazzini, R; Bissaldi, E; Blandford, RD; Bloom, ED; Bonino, R; Bottacini, E; Brandt, TJ; Bregeon, J; Bruel, P; Buehler, R; Caliandro, GA; Cameron, RA; Caputo, R; Caragiulo, M; Caraveo, PA; Cecchi, C; Charles, E; Chekhtman, A; Chiang, J; Chiaro, G; Ciprini, S; Claus, R; Cohen-Tanugi, J; Conrad, J; Cuoco, A; Cutini, S; D'Ammando, F; de Angelis, A; de Palma, F; Desiante, R; Digel, SW; Di Venere, L; Drell, PS; Drlica-Wagner, A; Essig, R; Favuzzi, C; Fegan, SJ; Ferrara, EC; Focke, WB; Franckowiak, A; Fukazawa, Y; Funk, S; Fusco, P; Gargano, F; Gasparrini, D; Giglietto, N; Giordano, F; Giroletti, M; Glanzman, T; Godfrey, G; Gomez-Vargas, GA; Grenier, IA; Guiriec, S; Gustafsson, M;

Hays, E; Hewitt, JW; Horan, D; Jogler, T; Jóhannesson, G; Kuss, M; Larsson, S; Latronico, L; Li, J; Li, L; Llena Garde, M; Longo, F; Loparco, F; Lubrano, P; Malyshev, D; Mayer, M; Mazziotta, MN; McEnery, JE; Meyer, M; Michelson, PF; Mizuno, T; Moiseev, AA; Monzani, ME; Morselli, A; Murgia, S; Nuss, E; Ohsugi, T; Orienti, M; Orlando, E; Ormes, JF; Paneque, D; Perkins, JS; Pesce-Rollins, M; Piron, F; Pivato, G; Porter, TA; Rainò, S; Rando, R; Razzano, M; Reimer, A; Reimer, O; Ritz, S; Sánchez-Conde, M; Schulz, A; Sehgal, N; Sgrò, C; Siskind, EJ; Spada, F; Spandre, G; Spinelli, P; Strigari, L; Tajima, H; Takahashi, H; Thayer, JB; Tibaldo, L; Torres, DF; Troja, E; Vianello, G; Werner, M; Winer, BL; Wood, KS; Wood, M; Zaharijas, G; Zimmer, S; Fermi-LAT Collaboration. "Searching for Dark Matter Annihilation from Milky Way Dwarf Spheroidal Galaxies with Six Years of Fermi Large Area Telescope Data," *Physical Review Letters*, v. 115(23), 2015, p. 231301. http://adsabs.harvard.edu/abs/2015PhRvL.115w1301A

[7] Adriani, O; Barbarino, GC; Bazilevskaya, GA; Bellotti, R; Bianco, A; Boezio, M; Bogomolov, EA; Bongi, M; Bonvicini, V; Bottai, S; Bruno, A; Cafagna, F; Campana, D; Carbone, R; Carlson, P; Casolino, M; Castellini, G; De Donato, C; De Santis, C; De Simone, N; Di Felice, V; Formato, V; Galper, AM; Karelin, AV; Koldashov, SV; Koldobskiy, SA; Krutkov, SY; Kvashnin, AN; Leonov, A; Malakhov, V; Marcelli, L; Martucci, M; Mayorov, AG; Menn, W; Mergé, M; Mikhailov, VV; Mocchiutti, E; Monaco, A; Mori, N; Munini, R; Osteria, G; Palma, F; Papini, P; Pearce, M; Picozza, P; Pizzolotto, C; Ricci, M; Ricciarini, SB; Rossetto, L; Sarkar, R; Scotti, V; Simon, M; Sparvoli, R; Spillantini, P; Stochaj, SJ; Stockton, JC; Stozhkov, YI; Vacchi, A; Vannuccini, E; Vasilyev, GI; Voronov, SA; Yurkin, YT; Zampa, G; Zampa, N; Zverev, VG. "Cosmic-Ray Positron Energy Spectrum Measured by PAMELA," *Physical Review Letters*, v. 111(8), 2013, p. 081102. http://adsabs.harvard.edu/abs/2013PhRvL.111h1102A

[8] Albert, A; Funk, S; Katagiri, H; Kawashima, T; Murphy, M; Okumura, A; Quagliani, R; Sapozhnikov, L; Shigenaka, A; Tajima, H; Tibaldo, L; Vandenbroucke, J; Varner, G; Wu, T. "TARGET 5: A new multi-channel digitizer with triggering capabilities for gamma-ray atmospheric Cherenkov telescopes," *Astroparticle Physics*, v. 92, 2017, p. 49–61. http://adsabs.harvard.edu/abs/2017APh....92...49A

[9] Atwood, WB; Abdo, AA; Ackermann, M; Althouse, W; Anderson, B; Axelsson, M; Baldini, L; Ballet, J; Band, DL; Barbiellini, G; et al. "The Large Area Telescope on the Fermi Gamma-Ray Space Telescope Mission," *Astrophysical Journal*, v. 697, 2009, p. 1071–1102. http://adsabs.harvard.edu/abs/2009ApJ...697.1071A

[10] Bechtol, K; Funk, S; Okumura, A; Ruckman, LL; Simons, A; Tajima, H; Vandenbroucke, J; Varner, GS. "TARGET: A multi-channel digitizer chip for very-high-energy gamma-ray telescopes," *Astroparticle Physics*, v. 36, 2012, p. 156–165. http://adsabs.harvard.edu/abs/2012APh....36..156B

[11] Binns, WR; Bose, RG; Braun, DL; Brandt, TJ; Daniels, WM; Dowkontt, PF; Fitzsimmons, SP; Hahne, DJ; Hams, T; Israel, MH; Klemic, J; Labrador, AW; Link, JT; Mewaldt, RA; Mitchell, JW; Moore, P; Murphy, RP; Olevitch, MA; Rauch, BF; Sakai, K; San Sebastian, F; Sasaki, M; Simburger, GE; Stone, EC; Waddington, CJ; Ward, JE; Wiedenbeck, ME. "The SUPERTIGER Instrument: Measurement of Elemental Abundances of Ultra-Heavy Galactic Cosmic Rays," *Astrophysical Journal*, v. 788, 2014, p. 18. http://adsabs.harvard.edu/abs/2014ApJ...788...18B

[12] Binns, WR; Israel, MH; Klarmann, J. "Scintillator-fiber charged-particle track-imaging detector," *Nuclear Instruments and Methods in Physics Research*, v. 216, 1983, p. 475–480. http://adsabs.harvard.edu/abs/1983NIMPR.216..475B

[13] Cherry, ML; Case, GL. "Compton scattered transition radiation from very high energy

particles," *Astroparticle Physics*, v. 18, 2003, p. 629–635. http://adsabs.harvard.edu/abs/2003APh....18..629C

[14] Cholis, I; Finkbeiner, DP; Goodenough, L; Weiner, N. "The PAMELA positron excess from annihilations into a light boson," *JCAP*, v. 12, 2009, p. 007. http://adsabs.harvard.edu/abs/2009JCAP...12..007C

[15] Cowsik, R; Burch, B; Madziwa-Nussinov, T. "The Origin of the Spectral Intensities of Cosmic-Ray Positrons," *Astrophysical Journal*, v. 786, 2014, p. 124. http://adsabs.harvard.edu/abs/2014ApJ...786..124C

[16] Davis, AJ; Hink, PL; Binns, WR; Epstein, JW; Connell, JJ; Israel, MH; Klarmann, J; Vylet, V; Kaplan, DH; Reucroft, S. "Scintillating optical fiber trajectory detectors," *Nuclear Instruments and Methods in Physics Research A*, v. 276, 1989, p. 347–358. http://adsabs.harvard.edu/abs/1989NIMPA.276..347D

[17] Freiburghaus, C; Rosswog, S; Thielemann, FK. "R-Process in Neutron Star Mergers," *Astrophysical Journal, Letters*, v. 525, 1999, p. L121–L124. http://adsabs.harvard.edu/abs/1999ApJ...525L.121F

[18] Funk, S; Jankowsky, D; Katagiri, H; Kraus, M; Okumura, A; Schoorlemmer, H; Shigenaka, A; Tajima, H; Tibaldo, L; Varner, G; Zink, A; Zorn, J. "TARGET: A digitizing and trigger ASIC for the Cherenkov telescope array," In *6th International Symposium on High Energy Gamma-Ray Astronomy*, v. 1792 of *American Institute of Physics Conference Series*, 2017, p. 080012. http://adsabs.harvard.edu/abs/2017AIPC.1792h0012F

[19] Goldstein, A; et al. "An ordinary short gamma-ray burst with extraordinary implications: Fermi -gbm detection of grb 170817a," *Astrophysical Journal, Letters*, v. 848(2), 2017, p. L14

[20] Hooper, D; Cholis, I; Linden, T; Fang, K. "HAWC observations strongly favor pulsar interpretations of the cosmic-ray positron excess," *Physics Review D*, v. 96(10), 2017, p. 103013. http://adsabs.harvard.edu/abs/2017PhRvD..96j3013H

[21] Ishimaru, Y; Wanajo, S; Prantzos, N. "Neutron Star Mergers as the Origin of r-process Elements in the Galactic Halo Based on the Sub-halo Clustering Scenario," *Astrophysical Journal, Letters*, v. 804, 2015, p. L35. http://adsabs.harvard.edu/abs/2015ApJ...804L..35I

[22] Just, O; Bauswein, A; Ardevol Pulpillo, R; Goriely, S; Janka, HT. "Comprehensive nucleosynthesis analysis for ejecta of compact binary mergers," *MNRAS*, v. 448, 2015, p. 541–567. http://adsabs.harvard.edu/abs/2015MNRAS.448..541J

[23] Komiya, Y; Shigeyama, T. "R-process Element Cosmic Rays from Neutron Star Mergers," *Astrophysical Journal*, v. 846, 2017, p. 143. http://adsabs.harvard.edu/abs/2017ApJ...846..143K

[24] Korobkin, O; Rosswog, S; Arcones, A; Winteler, C. "On the astrophysical robustness of the neutron star merger r-process," *MNRAS*, v. 426, 2012, p. 1940–1949. http://adsabs.harvard.edu/abs/2012MNRAS.426.1940K

[25] Kruskal, M; Ahlen, SP; Tarlé, G. "Secondary Production as the Origin of the Cosmic-Ray Positron Excess," *Astrophysical Journal*, v. 818, 2016, p. 70. http://adsabs.harvard.edu/abs/2016ApJ...818...70K

[26] Lapington, JS; Abchiche, A; Allan, D; Amans, JP; Armstrong, TP; Balzer, A; Berge, D; Boisson, C; Bousquet, JJ; Bose, R; Brown, AM; Bryan, M; Buchholtz, G; Buckley, J; Chadwick, PM; Costantini, H; Cotter, G; Daniel, MK; De Franco, A; De Frondat, F; Dournaux, JL; Dumas, D; Ernenwein, JP; Fasola, G; Funk, S; Gironnet, J; Graham, JA; Greenshaw, T; Hervet, O; Hidaka, N; Hinton, JA; Huet, JM; Jankowsky, D; Jegouzo, I; Jogler, T; Kawashima, T; Kraus, M; Laporte, P; Leach, S; Lefaucheur, J; Markoff, S; Melse,

T; Minaya, IA; Mohrmann, L; Molyneux, P; Moore, P; Nolan, SJ; Okumura, A; Osborne, JP; Parsons, RD; Rosen, S; Ross, D; Rowell, G; Rulten, CB; Sato, Y; Sayede, F; Schmoll, J; Schoorlemmer, H; Servillat, M; Sol, H; Stamatescu, V; Stephan, M; Stuik, R; Sykes, J; Tajima, H; Thornhill, J; Tibaldo, L; Trichard, C; Varner, G; Vink, J; Watson, JJ; White, R; Yamane, N; Zech, A; Zink, A; Zorn, J; CTA Consortium. "The GCT camera for the Cherenkov Telescope Array," *Nuclear Instruments and Methods in Physics Research A*, v. 876, 2017, p. 1–4. http://adsabs.harvard.edu/abs/2017NIMPA.876....1L

[27] Moiseev, AA; Ajello, M; Buckley, JH; Caputo, R; Ferrara, EC; Hartmann, DH; Hays, E; McEnery, JE; Mitchell, JW; Ojha, R; Perkins, JS; Racusin, JL; Smith, AW; Thompson, DJ. "Compton-Pair Production Space Telescope (ComPair) for MeV Gamma-ray Astronomy," preprint (arXiv:1508.07349), 2015. http://adsabs.harvard.edu/abs/2015arXiv150807349M

[28] Moskalenko, IV; Strong, AW. "Production and Propagation of Cosmic-Ray Positrons and Electrons," *Astrophysical Journal*, v. 493, 1998, p. 694–707. http://adsabs.harvard.edu/abs/1998ApJ...493..694M

[29] Prantzos, N; Abia, C; Limongi, M; Chieffi, A; Cristallo, S. "Chemical evolution with rotating massive star yields I. The solar neighborhood and the s-process elements," *MNRAS*, 2018. http://adsabs.harvard.edu/abs/2018MNRAS.tmp..302P

[30] Rauch, BF; Link, JT; Lodders, K; Israel, MH; Barbier, LM; Binns, WR; Christian, ER; Cummings, JR; de Nolfo, GA; Geier, S; Mewaldt, RA; Mitchell, JW; Schindler, SM; Scott, LM; Stone, EC; Streitmatter, RE; Waddington, CJ; Wiedenbeck, ME. "Cosmic Ray origin in OB Associations and Preferential Acceleration of Refractory Elements: Evidence from Abundances of Elements $_{26}$Fe through $_{34}$Se," *Astrophysical Journal*, v. 697, 2009, p. 2083–2088. http://adsabs.harvard.edu/abs/2009ApJ...697.2083R

[31] Shibagaki, S; Kajino, T; Mathews, GJ; Chiba, S; Nishimura, S; Lorusso, G. "Relative Contributions of the Weak, Main, and Fission-recycling r-process," *Astrophysical Journal*, v. 816, 2016, p. 79. http://adsabs.harvard.edu/abs/2016ApJ...816...79S

[32] Stacy, JG; Kippen, RM; Kappadath, SC; McConnell, M; Morris, D; Miller, R; Connors, A; Hersh, B; Ryan, J; Macri, J; Simpson, G; Schoenfelder, V; Steinle, H; van Dijk, R; Williams, OR. "The response of the CGRO COMPTEL determined from Monte Carlo simulation studies.," *AAPS*, v. 120, 1996, p. 691–694. http://adsabs.harvard.edu/abs/1996A\%26AS..120C.691S

[33] Stone, EC; Cohen, CMS; Cook, WR; Cummings, AC; Gauld, B; Kecman, B; Leske, RA; Mewaldt, RA; Thayer, MR; Dougherty, BL; Grumm, RL; Milliken, BD; Radocinski, RG; Wiedenbeck, ME; Christian, ER; Shuman, S; Trexel, H; von Rosenvinge, TT; Binns, WR; Crary, DJ; Dowkontt, P; Epstein, J; Hink, PL; Klarmann, J; Lijowski, M; Olevitch, MA. "The Cosmic-Ray Isotope Spectrometer for the Advanced Composition Explorer," *Space Sciences Research*, v. 86, 1998, p. 285–356. http://adsabs.harvard.edu/abs/1998SSRv...86..285S

[34] Tibaldo, L; Vandenbroucke, J; Albert, A; Funk, S; Kawashima, T; Kraus, M; Okumura, A; Sapozhnikov, L; Tajima, H; Varner, G; Wu, T; Zink, A. "TARGET: toward a solution for the readout electronics of the Cherenkov Telescope Array," In *34th International Cosmic Ray Conference (ICRC2015)*, v. 34 of *International Cosmic Ray Conference*, 2015, p. 932. http://adsabs.harvard.edu/abs/2015ICRC...34..932T

[35] Tome, S; et al. " ," In *SciFi-93-Workshop on Scintillating Fiber Detectors, Ed. Bross, Ruchti and Wayne, Pub. World Scientific*, 1993, p. 450

[36] Torii, S; CALET Collaboration. "The CALET mission for detection of cosmic ray sources and dark matter," In *Journal of Physics Conference Series*, v. 120 of *Jour-*

nal of Physics Conference Series, 2008, p. 062020. http://adsabs.harvard.edu/abs/2008JPhCS.120f2020T

[37] Torii, S; Shimizu, Y; Kasahara, K; Hasebe, N; Hareyama, M; Kodaira, S; Okudaira, O; Yamashita, N; Miyazima, M; Miyaji, T; Tkayangai, M; Ueno, S; Tomida, H; Saito, Y; Fuke, H; Yamagami, T; Nishimura, J; Tamura, T; Tateyama, N; Hibino, K; Okuno, S; Shiomi, A; Takita, M; Yuda, T; Kakimoto, F; Tsunesada, Y; Terasawa, T; Kobayashi, T; Yoshida, A; Yamaoka, K; Katayose, Y; Shibata, M; Ichimura, M; Kuramata, S; Uchihori, Y; Kitamura, A; Yoshida, K; Murakami, H; Komori, Y; Mizutani, K; Munakata, K; Streitmatter, RE; Mitchell, JW; Barbier, LM; Moiseev, AA; Krizmanic, JF; Ormes, JF; Wefel, JP; Case, G; Cherry, ML; Guzik, TG; Isbert, JB; Binns, WR; Israel, MH; Krawczynski, HS; Marrocchesi, PS; Bigongiari, G; Batkov, K; Kim, MY; Bagliesi, MG; Masestro, P; Millucci, V; Zei, R; Adriani, O; Papini, P; Vannuccini, E; Bonechi, L; Chang, J; Yan, J; Gan, W. "The CALET Mission on International Space Station," *International Cosmic Ray Conference*, v. 2, 2008, p. 393–396. http://adsabs.harvard.edu/abs/2008ICRC....2..393T

[38] Valls, J; et al. " ," In *SciFi-97-Conference on Scintillating and Fiber Detectors, Ed. Bross, Ruchti and Wayne*, v. 450 of *AIP Conference Proceedings*, 1993, p. 229

[39] van de Voort, F; Quataert, E; Hopkins, PF; Kereš, D; Faucher-Giguère, CA. "Galactic r-process enrichment by neutron star mergers in cosmological simulations of a Milky Way-mass galaxy," *MNRAS*, v. 447, 2015, p. 140–148. http://adsabs.harvard.edu/abs/2015MNRAS.447..140V

[40] Varner, GS; Ruckman, LL; Nam, JW; Nichol, RJ; Cao, J; Gorham, PW; Wilcox, M. "The large analog bandwidth recorder and digitizer with ordered readout (LABRADOR) ASIC," *Nuclear Instruments and Methods in Physics Research A*, v. 583, 2007, p. 447–460. http://adsabs.harvard.edu/abs/2007NIMPA.583..447V

[41] Wakely, SP. "Precision X-ray transition radiation detection," *Astroparticle Physics*, v. 18, 2002, p. 67–87. http://adsabs.harvard.edu/abs/2002APh....18...67W

[42] Wanajo, S. "The r-process in Proto-neutron-star Wind Revisited," *Astrophysical Journal, Letters*, v. 770, 2013, p. L22. http://adsabs.harvard.edu/abs/2013ApJ...770L..22W

[43] Wanajo, S; Sekiguchi, Y; Nishimura, N; Kiuchi, K; Kyutoku, K; Shibata, M. "Production of All the r-process Nuclides in the Dynamical Ejecta of Neutron Star Mergers," *Astrophysical Journal, Letters*, v. 789, 2014, p. L39. http://adsabs.harvard.edu/abs/2014ApJ...789L..39W

[44] Wu, MR; Fernández, R; Martínez-Pinedo, G; Metzger, BD. "Production of the entire range of r-process nuclides by black hole accretion disc outflows from neutron star mergers," *MNRAS*, v. 463, 2016, p. 2323–2334. http://adsabs.harvard.edu/abs/2016MNRAS.463.2323W